

Evaluation of ICE and capacitive decoupling methods using in 8-channel loop array coils at 7T

Xinqiang Yan^{1,2}, Xiaoliang Zhang^{3,4}, Chuangxin Ma², Long Wei², and Rong Xue¹

¹State Key Laboratory of Brain and Cognitive Science, Beijing MRI Center for Brain Research, Institute of Biophysics, Chinese Academy of Sciences, Beijing, Beijing, China, ²Key Laboratory of Nuclear Analysis Techniques, Institute of High Energy Physics, Chinese Academy of Sciences, Beijing, Beijing, China, ³Department of Radiology and Biomedical Imaging, University of California San Francisco, San Francisco, California, United States, ⁴UCSF/UC Berkeley Joint Graduate Group in Bioengineering, San Francisco, California, United States

INTRODUCTION

Phased array coils have been widely used for better SNR in high field MRI, and various methods were employed to reduce the mutual coupling between coil elements [1-3]. A new decoupling method based on induced current compensation or elimination (ICE) for microstrip line planar array has been proposed recently [4-6], showing the capability of reducing the strongly coupled resonant elements. In this study, two eight-channel transmit/receive volume-type loop-array coils were built for human head imaging at 7T by using the ICE decoupling method and capacitive decoupling method, respectively. We investigated the ICE decoupling method and the capacitive decoupling method in terms of the S-parameter matrix, SNR and parallel imaging capability.

MATERIALS and METHODS

Both coils were built on a cylindrical acrylic former with an outer diameter of 25cm (Fig. 1). Rectangular loops (length 17cm, width 6.8cm) with six equally distributed capacitors were used as the coil elements. The width of the conductor is 5mm and the thickness is 100 μ m. Both coils were used for transmission and reception, matched to 50 Ω and tuned to 297.2MHz, which was the proton Larmor frequency of our 7T MRI system. For the ICE-decoupled array, one smaller rectangular loop (length 17cm, width 2.8cm) was placed between adjacent coil elements to reduce the mutual coupling. For the conventional capacitively decoupled array, a pair of capacitors was used to remove the coupling between adjacent coil elements [2, 7-8]. S-parameter matrices of both arrays were measured with an Agilent E5071C network analyzer. GRE images of the two arrays in the transverse plane with same parameters were shown for signal-to-noise (SNR) comparison. Imaging parameters used were: FA=25deg, TR=120ms, TE=6ms, FOV=250 \times 250 mm², Matrix=256 \times 256, ST (Slice Thickness)=5mm, Bandwidth=320Hz/pixel. All MRI experiments for phantom and human head studies were performed on a whole-body MRI scanner (7T MAGNETOM, Siemens Healthcare, Erlangen, Germany). The image SNR was determined by a previously reported method [9]. In the SNR measurements, signal came from a square of 20 \times 20 pixels in each of the five positions at the center and periphery of the image. G-factor maps in the sagittal plane with reduction factors of 2, 3 and 4 using GRAPPA of both arrays were also shown to demonstrate their capabilities for parallel imaging. The g-factor maps and average g-factors were calculated by using a RF coil array design software Musaik (Speag, Switzerland).

RESULTS

S-parameter matrices of the 8-channel ICE-decoupled loop array and capacitively decoupled loop array loaded with human head were measured as shown in Fig. 2. Average S21 between two adjacent elements of the ICE-decoupled array and capacitively decoupled array were -26.9dB and -16.4dB, respectively. For the ICE-decoupled array, the average Q_{UL} and Q_L of a single element were 120 and 49, respectively. For the capacitively decoupled array, the average Q_L of a single element was 40. Q_{UL} can't be calculated because the resonance peak split when unloading. Fig. 3 shows the combined GRE images of both arrays. Local SNR at four peripheral areas and the center of brain were calculated and marked on the images. Compared with the capacitively decoupled array, the ICE-decoupled array has an overall SNR gain of 13% because of its better decoupling performance. G-factor maps of both arrays obtained with reduction factors R of 2, 3, and 4 in the sagittal plane were shown Fig. 4. Average g-factors of both arrays with R=2, 3 and 4 are marked in the g-factor maps. The g-factors of the ICE-decoupled array were relatively smaller or better, especially for high reduction factor, e.g., R=4. This indicates that better image quality with fast imaging can be achieved by using the ICE-decoupled transmitter coil array over conventional capacitively decoupled array.

DISCUSSION and CONCLUSION

Comparing with the conventional capacitively decoupled array, the ICE-decoupled array has much better isolation between adjacent coil elements. Due to its better decoupling performance and higher Q_{UL} , the ICE-decoupled array has higher SNR compared with the capacitively decoupled loop array, with an overall gain of 13%. The ICE-decoupled array also showed better parallel imaging capability that the average g-factor of human head in the sagittal plane was only 1.14 when the reduction or acceleration factor achieves 4. This improvement can also be verified by the comparison of S-parameter matrices as described above. Additionally, the ICE decoupling method is more robust that decoupling loops do not need to be retuned for different loads. Furthermore, the ICE-decoupled array has no physical connection between the decoupling loops and coil array elements, which provides a mechanically robust structure for flexible transmitter arrays.

ACKNOWLEDGEMENTS

This work was supported by the Ministry of Science and Technology of China Grant (2012CB825500), Chinese National Major Scientific Equipment R&D Project (Grant No. ZDYZ2010-2) and National Natural Science Foundation of China Grant (51228702).

REFERENCES

[1] P. B. Roemer, et al, Magn Reson Med, vol. 16, pp. 192-335, 1990. [2] C. Von Morze, et al, Concept Magn Reson B, vol. 31B, pp. 37-43, 2007. [3] N. I. Avdievich, Appl Magn Reson, vol. 41, pp. 483-506, 2011. [4] Y. Li, et al, Medical Physics, vol. 38, pp. 4086-93, 2011. [5] Z. Xie, et al, Proc. ISMRM, p. 1068, 2008. [6] Z. Xie, et al, Proc. ISMRM, p. 2973, 2008. [7] Z. Zuo, et al, Proc. ISMRM, p. 2804, 2012. [8] H. Jeong, et al, Proc. ISMRM, p. 4351, 2013. [9] J. T. Vaughan, et al, Magn Reson Med, vol. 24, pp. 24-30, 2001.

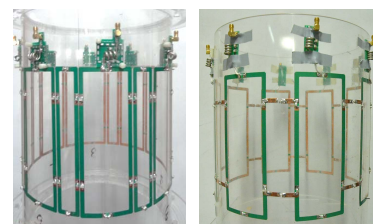


Figure 1: Photographs of the 8-channel ICE-decoupled loop array (left) and capacitively decoupled loop array (right).

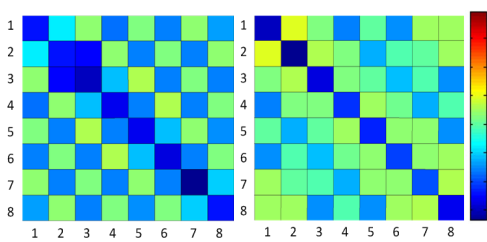


Figure 2: S-parameter matrices of the 8-channel ICE-decoupled array (left) and capacitively decoupled array (right).

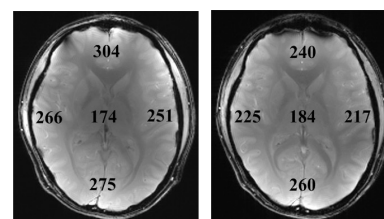


Figure 3: GRE images of the 8-channel ICE-decoupled array (left) and capacitively decoupled array (right) in the transverse plane.

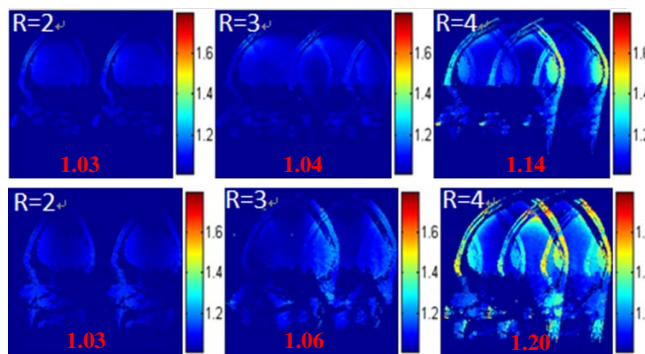


Figure 4: G-factor maps of ICE-decoupled array (top row) and capacitively decoupled array (bottom row) with accelerate factors R of 2, 3 and 4 in the sagittal plane. Average g-factors of both arrays with R=2, 3 and 4 are marked in red color.